Regularity and randomness in ageing: Differences in resting-state EEG complexity measured by largest Lyapunov exponent

Matthew King-Hang Ma [a],[*], Manson Cheuk-Man Fong [b], Chenwei Xie [b], Tan Lee [a], Guanrong Chen [c], William Shiyuan Wang [a],[b],[d],[**]

[a] *Department of Electronic Engineering, The Chinese University of Hong Kong, Hong Kong*
[b] *Research Centre for Language, Cognition, and Neuroscience, Department of Chinese and Bilingual Studies, The Hong Kong Polytechnic University, Hong Kong*
[c] *Department of Electrical Engineering, City University of Hong Kong, Hong Kong*
[d] *Research Institute for Smart Aging, The Hong Kong Polytechnic University, Hong Kong*

ARTICLE INFO

ABSTRACT

The loss of complexity in ageing hypothesis (LOCH) has found support from EEG studies, most of which adopted signal-domain complexity measures. The present study adopted the largest Lyapunov exponent (LLE) to measure complexity from a nonlinear dynamical systems perspective. A total of 144 participants were included and divided into young, young-old and old-old groups. Both sensor-space and source-space results showed significantly lower LLE for older than younger adults. The age-related differences were region-dependent, being most prominent in the frontal region, followed by bilateral temporal regions. The occipital region showed non-significant differences. Significant reduction of LLE in the posterior cingulate was also observed by virtue of the source-space analysis. We also evaluated the relationships between LLE and other complexity measures. The most intriguing result was the negative correlation between LLE and Lempel-Ziv complexity (LZC). The age-related decrease in LLE indicated a higher regularity in dynamics, while the higher LZC indicated a higher randomness in the signal domain. The new findings support the LOCH by demonstrating the simultaneous increase in regularity and randomness.

1. Introduction

Ageing is usually accompanied by deficits in functional components and alterations of interactions between these components (Lipsitz and Goldberger, 1992), and has been described as a consequence of reduced physiological complexity in all levels, including molecular, cellular, organismic and behavioral (Kyriazis, 2003; Sehl and Yates, 2001). The loss of complexity in ageing hypothesis (LOCH) postulates that the deterioration above is manifested by the decrease in complexity in the physiological signals (Lipsitz and Goldberger, 1992; Sleimen-Malkoun et al., 2014).

The development of LOCH was closely related to the emergence of chaos theory. To investigate how the LOCH is manifested in the ageing brain, techniques from nonlinear dynamics were applied to identify the presence of chaos in EEG signals (Pritchard et al., 1991; Meyer-Lindenberg, 1996; Anokhin et al., 1996). The presence of chaotic activities

suggests nonlinear interactions among functional components, which is a sign of healthy physiologic function and indicates brain plasticity (Coffey, 1998; Goldberger et al., 2002a). Early studies suggested a linear increase in complexity in developmental stages, from childhood to adulthood and to old age (up to age of 60) (Meyer-Lindenberg, 1996; Anokhin et al., 1996). Higher spatial complexity was reported in older than younger adults in cross-sectional studies (Pierce et al., 2000, 2003). However, there were also opposite findings (Pritchard et al., 1991; Bruce et al., 2009). Dimensional complexity and nonlinear coupling were found to be in opposite relationship (Meyer-Lindenberg, 1996; Müller and Lindenberger, 2012), suggesting the heterogeneity of different complexity measures. Later studies with extended age range from childhood to the age of 80s revealed a more complicated trajectory, showing inverted U-shaped trends of complexity that peak around the age of 60s (Fernández et al., 2012; Zappasodi et al., 2015; Shumbayawonda et al., 2018).

Although there exists a decent number of studies on complexity, a great variety of complexity measures was adopted, raising the difficulties in interpretations and comparisons. Early measures including correlation dimension (CD) (Pritchard et al., 1991) and the largest Lyapunov exponent (LLE) (Adeli et al., 2007; Khoa et al., 2012; Dauwels et al., 2011; Jeong, 2004) were stemmed from chaos and nonlinear dynamics theory. Information theory based measures like sample entropy (SampEn) (Bruce et al., 2009; Richman and Moorman, 2000; Jia et al., 2017) and Lempel-Ziv complexity (LZC) (Fernández et al., 2012; Shumbayawonda et al., 2018; Lempel and Ziv, 1976; Aboy et al., 2006; McBride et al., 2014) have been gaining popularity in recent years due to their relatively low computational cost. In the spectral domain, the presence of a 1/f slope in the power spectrum is also a characteristic of a complex system, and has been related to ageing (He et al., 2010; Voytek et al., 2015). However, measures stemmed from nonlinear dynamics are fundamentally different from others in the sense that they are derived by assuming the existence of a dynamical system that describes the dynamics of EEG signals. Although the true dynamics may never be known, one could apply the Takens's Embedding theorem to reconstruct a topologically equivalent state space and corresponding dynamics (Takens, 1981; Krakovská et al., 2015). As such, topologically invariant measures like CD and LLE can be estimated from the reconstructed dynamics. In contrast, other measures like SampEn and LZC directly operate on the signal domain, without assuming an underlying nonlinear dynamical system. Therefore, it is questionable if the complexity inferred by these different measures are describing the same construct.

Another important issue is the multiple synonyms of complexity found in the literature. In many studies, complexity has been made synonymous with "variability", "irregularity", "randomness", etc. (Fernández et al., 2012; Shumbayawonda et al., 2018; Jia et al., 2017; Jeong et al., 2001; Abásolo et al., 2006). When LOCH was proposed, complexity was defined as the extent to which the underlying system generates aperiodic fluctuations that resemble nonlinear chaos (Lipsitz and Goldberger, 1992; Goldberger et al., 2002a). The breakdown of complexity could lead to the emergence of a characteristic frequency, or completely uncorrelated randomness (Goldberger et al., 2002a; Lipsitz, 2004). As such, increasing randomness could lead to both increase or decrease in complexity. In short, complexity describes a state between order and disorder (Chialvo, 2018). Treating these terms equally is akin to picking one side of the story and may cause confusions.

The present study has two major objectives. The first is to evaluate the LOCH in EEG signals via the LLE. Although LLE is an "old" measure that has been investigated in the diagnosis of various diseases such as epilepsy (Adeli et al., 2007), Parkinson's disease and dementia (Jeong, 2004; Jeong et al., 1998, 2001; Stam et al., 1994, 1995; 1995), the modulation of LLE in normal ageing has remained unclear. To our knowledge, only one study has reported the decrease of LLE in frontal regions from infancy to adulthood (Meyer-Lindenberg, 1996). The second objective is to investigate the age-related trends of other complexity measures that quantify complexity from the signal domain, and the relationships between LLE and these measures.

2. Methods

2.1. Data collection

145 participants that were native Cantonese speakers without known neurological disorders were recruited. Younger adults were undergraduate or postgraduate students recruited from Hong Kong Polytechnic University, older adults (age $\geq$60) were recruited via the Prince of Wales hospital and the Institute of Active Ageing in Hong Kong Polytechnic University. All older adults underwent the Montreal Cognitive Assessment Hong Kong Version (Wong et al., 2009) and were identified as cognitive normal according to the 7th percentile cutoff of normative data, after adjustment for education years (Wong et al., 2015).

Three minutes of resting-state EEG in eyes-open and eyes-closed condition were collected for each participant. EEG signals were acquired using a 32-channel BioSemi ActiveTwo System with Ag/AgCl electrodes, digitized at a sampling rate of 2048Hz. Horizontal and vertical electrooculograms (HEOG and VEOG) were recorded using two pairs of electrode placing near the two outer canthi and above or below the left eye respectively. Participants sat comfortably about 70 cm in front of a monitor. In the eyes-open condition, participants were asked to fixate on a cross at the center of the screen. In eyes-closed condition, participants were asked to relax and avoid any movements. Both conditions were recorded in a dim room. Written signed informed consent was obtained from all participants. All experimental procedures were approved by the Ethical Review Committee, Hong Kong Polytechnic University.

2.2. Preprocessing of EEG signals

The signal processing algorithms were implemented using custom scripts in Python with the MNE-Python library (Gramfort et al., 2013). The acquired EEG signals were downsampled to 512 Hz, band-pass filtered from 1 to 45 Hz, and average referenced. Independent component analysis (ICA) was applied to remove eye artifacts. Specifically, Spearman correlation was computed between each extracted independent component and the VEOG/HEOG. The correlation values were transformed to z-scores, and the components z-score values higher than 3.0 were excluded. After eyes artifacts removal, the EEG signals were visually inspected to filter out signals that are contaminated by body movements which are several orders of magnitude larger than the EEG signal. One participant was excluded from the study, resulting in 144 participants in total in the statistical analyses. Their demographic information will be described in later sections.

2.3. Extracting complexity measures

The present study included 4 different complexity measures: largest Lyapunov exponent (LLE), Lempel-Ziv complexity (LZC), 1/f slope of power spectrum (1/f slope) and the sample entropy (SampEn). Fig. 1 provides an overview of the four selected measures and highlights the differences between LLE and the other complexity measures. Each complexity measure was computed for each channel and participant. The complexity values from 32 channels were averaged over 6 scalp regions, as shown in Fig. 2a: Prefrontal (FP: Fp1, Fp2, AF3, AF4); frontocentral (FC: F3, Fz, F4, FC1, FC2); centroparietal (CP: C3, Cz, C4, CP1, CP2, P3, Pz, P4); parieto-occipital (PO: PO3, PO4, O1, Oz, O2); left temporal (LT: F7, FC5, T7, CP5, P7) and right temporal (RT: F8, FC6, T8, CP6, P8). These scalp regions will be referred as *sites* hereafter to emphasize the fact that we are referring to the sensor-space but not the source-space.

2.3.1. Largest Lyapunov exponent (LLE)

Various methods were proposed for computing the largest Lyapunov exponent, including Wolf's method (Wolf et al., 1985), Rosenstein's method (Rosenstein et al., 1993), etc. The present study adopted Rosenstein's method as it requires much less data points, is faster to compute and is more robust to noise as compared with Wolf's method. Prior to computing LLE, Takens's delay-embedding method was applied to embed the target signal into a state space of specified embedding dimension (Takens, 1981). After reconstructing the dynamics, the nearest neighbor of each point in the trajectory is identified. As the system evolves over time, the distance between each point and its nearest neighbor increases exponentially. An illustration is given as in Fig. 1a–c. Mathematically, for each point and its nearest neighbor, the divergence of their distance can be expressed as:

$$d(i) \approx C e^{\lambda_1 (i\Delta t)} \tag{1}$$
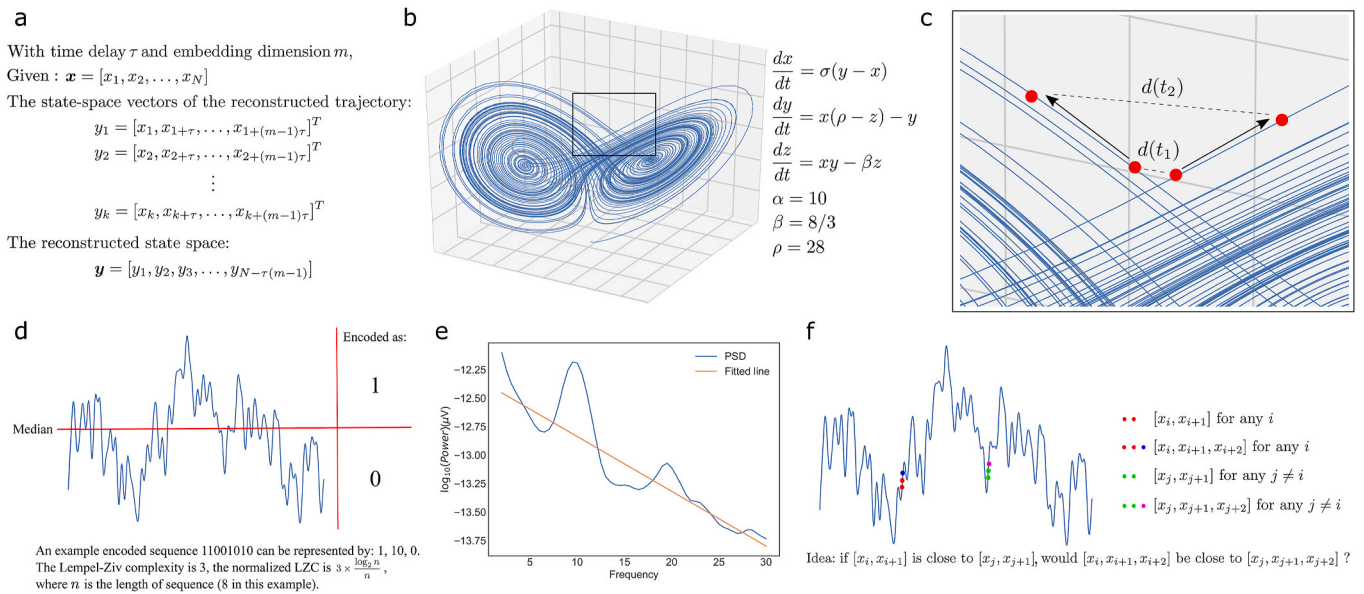
Fig. 1. Illustrations on the four complexity measures investigated in this study. This set of figures attempts to point out the differences between LLE and other measures in the sense that LLE is computed in the embedded state space but other measures are not. **a,** Description of the delay-embedding. Given a time series x of length N. A new, multivariate time series of dimension m is formed by vectors $y_i = [y_i, y_{i+1}, …, y_{i+(m-1)\tau}]$ for $i = 1, …, N - \tau(m - 1)$, each y_i is a state vector of the reconstructed state space. **b,** Left: The reconstructed state space of a Lorenz system as an example. Right: The corresponding Lorenz system equations. **c,** the enlarged part of the black square in **b.** The two red dots represent a random pair of point and its nearest neighbor, $d(t_1)$ is the distance between them at time t_1. When time evolves to t_2, the distance between the two points increase exponentially. The LLE describes the mean divergence rate over all pairs of such combinations. **d,** A demonstration on the calculation of LZC. A signal is binarized into sequence of 0s and 1s according to its median. The number of subsequences needed to represent the whole sequence is calculated by the algorithm. **e,** A demonstration on the calculation of $1/f$ slope. The blue line represent the PSD of the Pz channel in the log scale from one of the participants. The orange line is fitted via linear regression with the PSD from 2 to 30 Hz excluding the alpha band (8–13 Hz). The $1/f$ slope is the slope of the fitted line. **f,** An intuitive explanation on the idea of the sample entropy. By selecting two random points x_i and x_j on the signal, the question to be asked is if $[x_i, x_{i+1}]$ is close to $[x_j, x_{j+1}]$, would $[x_i, x_{i+1}, x_{i+2}]$ be close to $[x_j, x_{j+1}, x_{j+2}]$ too? A higher probability corresponds to lower sample entropy. (For interpretation of the references to colour in this figure legend, the reader is referred to the Web version of this article.)
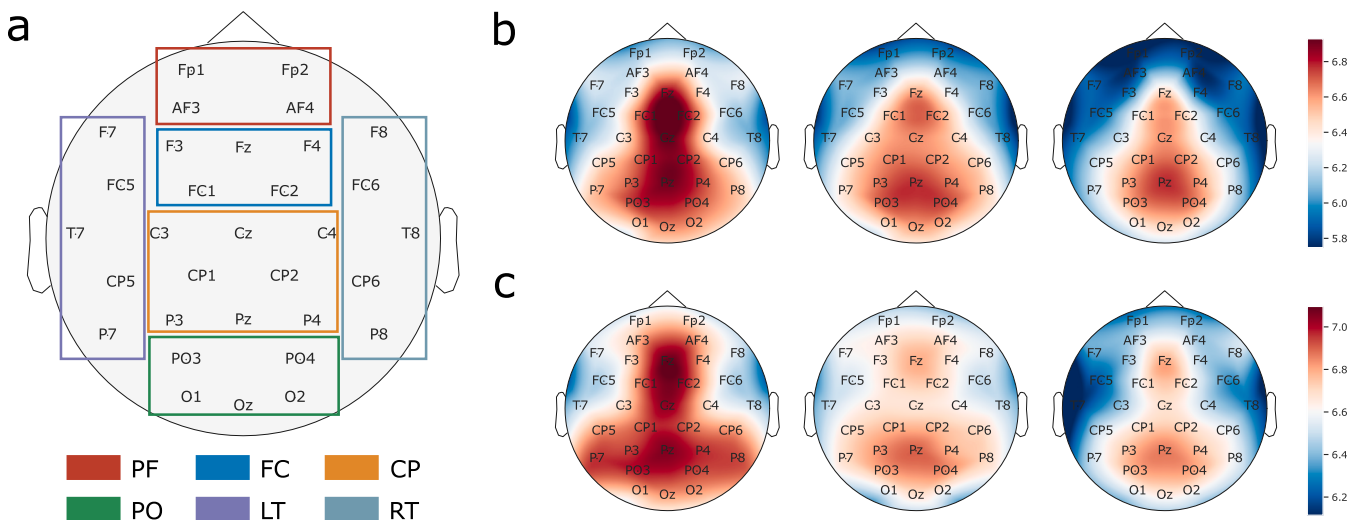
Fig. 2. The scalp regions defined and the grand-averaged LLE topographies. **a,** the 32-channel montage used in the present study. The channels were grouped into 6 scalp regions (referred as site in the main text): prefrontal (FP: Fp1, Fp2, AF3, AF4); frontocentral (FC: F3, Fz, F4, FC1, FC2); centroparietal (CP: C3, Cz, C4, CP1, CP2, P3, Pz, P4); parieto-occipital (PO: PO3, PO4, O1, Oz, O2); left temporal (LT: F7, FC5, T7, CP5, P7) and right temporal (RT: F8, FC6, T8, CP6, P8). **b,** The LLE topographies in eyes-open condition, averaged within age group. **c,** The LLE topographies in eyes-closed condition, averaged within age group.

where C, i and Δt are the initial separation between neighbors, index of time step and sampling period respectively. Applying logarithm on equation (1), one has:

$$\ln d(i) \approx \ln C + \lambda_1(i\Delta t) \qquad (2)$$

The LLE is approximated as the average rate of divergence across all pairs of points and their corresponding nearest neighbors. To determine suitable delay and embedding dimension of EEG signals, the recommendation is to estimate the delay first, and followed by the estimation of embedding dimensions (Krakovská et al., 2015; Adeli et al., 2007). Initially, the delay was determined by the first local minimum of the mutual information between delayed components of the EEG signal (Supplementary Fig. S1a). The embedding dimension was then

determined using the Cao's method (Cao, 1997) (Supplementary Fig. S1b), the dimension in which the changes of average distances between nearest neighbors approach to 0 was chosen. The choices of delay and embedding dimension were 19 and 20. Since the computation of LLE requires a linearly increasing region in the average divergence between nearest neighbors against time (Rosenstein et al., 1993), the divergence plot was visualized and checked accordingly. However, for delay equal to 19, no linear increasing region but oscillating behavior was found in the divergence plot (Supplementary Fig. S1c), similar to the example shown in the study that introduced the Rosenstein's algorithm (see Figure 6 of Rosenstein et al., 1993) when the delay parameter was too extreme. As such, we then tried to lower the value of delay until the average divergence curve no longer exhibited oscillating behaviors. Finally, the second largest delay parameter which did not result in oscillating behaviors was chosen as it would be more conservative and thus guard against potential oscillating behaviors in the divergence curve (Supplementary Fig. S1d). The final choices of delay and embedding dimension were 4 and 20, respectively. The same parameters were applied across all participants to reduce variances originated from the parameter choices.

However, there exists ambiguity in identifying the linear region. In this study, we adopted the following process to compute the slope. A sliding window of 5 samples ($\approx 0.01s$) and stride of 1 sample was applied to compute multiple slope instances. The LLE was estimated as the average slope. Slopes of absolute values below 1 were excluded from the computation in order to avoid the saturated flat region that might lead to underestimation of the average slope.

2.3.2. Lempel-Ziv complexity (LZC)

The computation of the LZC followed the original algorithm developed in 1976 (Lempel and Ziv, 1976). The first step is to convert the target signal (the EEG signal) into a symbolic, binary string. The operation can be written as:

$$c(t) = \begin{cases} 1, & \text{if } s(t) > T \\ 0, & \text{otherwise} \end{cases} \quad (3)$$

where $c(t)$, ($s(t)$ and T are the derived binary sequence, the original signal and a pre-defined threshold (equal to the median in the present study) respectively. The resultant string is then parsed from left to right and the LZC is defined as the number of distinct patterns identified. Consider the example sequence be 11001010. The algorithm would identify 3 distinct segments as 1.10.0 such that the 3 segments can effectively represent the whole sequence. The LZC of the sequence is 3. However, the resulted LZC depends on the length of the sequence. An normalized version of LZC, which is independent of sequence length, is expressed as (Fernández et al., 2012):

$$C_{norm} = C_{raw} \frac{\log_2 n}{n} \quad (4)$$

where n is the signal length and C_{raw} and C_{norm} are the raw and normalized LZC respectively. The above process is illustrated in Fig. 1d. LZC hereafter refers to the normalized LZC. While often being interpreted as a complexity measure (Fernández et al., 2012; Shumbayawonda et al., 2018), LZC was originally proposed to reflect randomness (Lempel and Ziv, 1976).

2.3.3. 1/f slope

Prior to the calculation of 1/f slope, the EEG signals were segmented into 2-s epochs. Epochs with exceptionally high peak-to-peak amplitude (z-score > 3) were excluded. The power spectral density of each epoch was computed using Welch's method (50% overlapped Hamming window and 1024-point FFT). The 1/f slope was calculated by fitting linear regression on log power against frequency on the averaged PSD. The frequency range to calculate the 1/f slope was between 2 and 30 Hz and alpha band (8–13 Hz) was excluded from the fitting following a previous

study (Voytek et al., 2015). An example is shown in Fig. 1e. The 1/f slope was suggested to reflect the neural noise (Voytek et al., 2015). A flatter slope (less negative) might indicate a lower signal-to-noise ratio in neuronal communications (Voytek et al., 2015; Cremer and Zeef, 1987).

2.3.4. Sample entropy (SampEn)

To calculate SampEn, we need to define a length m for extracting template vectors and a threshold r to determine if a pair of template vectors are close to each other. The SampEn is the negative log probability of two close (Chebyshev distance between vectors less than a threshold d) template vectors ($x_m(i)$, $x_m(j)$) remaining close when the length of the template vectors m is increased by 1 ($x_{m+1}(i)$, $x_{m+1}(j)$). A simplified illustration is shown in Fig. 1f. Let $A^m(r)$ and $B^m(r)$ be the probability that a pair of template vectors of length m and $m + 1$ are close to each other respectively. The SampEn is defined as (Richman and Moorman, 2000):

$$-ln\left(\frac{A^m(r)}{B^m(r)}\right) \quad (5)$$

In the present study, m was chosen as 2 and r was chosen as 0.2 times the standard deviation of the target EEG signal, following similar parameters used in previous studies (Abásolo et al, 2005, 2006). A larger SampEn is generally interpreted as higher irregularity or complexity (Bruce et al., 2009; Jia et al., 2017).

2.4. Statistical analysis

The statistical analysis comprised two parts. First of all, the 144 participants were divided into three age groups: young ($n = 55$ (30F), mean age 21.5 ± 2.07, range $18.1 - 26.0$), young-old ($n = 62$ (40F), mean age 65.7 ± 2.97, range $60.1 - 69.9$) and old-old ($n = 27$ (12F), mean age 73.8 ± 3.89, range $70.0 - 85.9$). A 3-way $3 \times 6 \times 2$ mixed ANOVA (age group: young, young-old and old-old; site: PF, FC, CP, PO, LT and RT; eyes condition: open and closed) was fitted with gender (female or male) as a covariate. The age group was a between-subject factor, while site and eyes condition were within-subject factors. The model was fitted with the R (R Core Team, 2020) package lme4 (Bates et al., 2015). The Q-Q plot of the dependent variable (LLE) and the residuals versus fits plot of the fitted models were visually inspected. Significant main and interaction effects were investigated post hoc with ANOVA and 2-sided pairwise t-test with estimated marginal means (Lenth, 2020). Greenhouse-Geisser correction was applied if the sphericity assumption was not met. Multiple comparisons were corrected by Holm's method (Holm, 1979).

The second part was correlation analysis to assess the relationship between complexity measures and age, as well as the relationship between different complexity measures. Firstly, the Spearman rank correlations between each complexity measure with age were calculated to reveal the age-related trend. The correlation was calculated separately for the young and old group (merging young-old and old-old group). Secondly, the correlation and partial correlation between each pair of the four complexity measures were computed for each age group to reveal how different complexity measures were related with each other. All correlation results were corrected for multiple comparisons by Holm's method (Holm, 1979).

In addition to the main analysis on age-related differences in complexity, the relationship between EEG alpha activities and LLE was examined to guard against the possibility that any age-related difference observed could be explained by the alpha activities (alpha power and alpha blocking effect). To calculate the alpha power, the EEG signals were first segmented into 2-s epochs and then the power spectral density (PSD) of each 2-s epoch was calculated using the Welch's method (with 50% overlapped Hamming window and 1024-point FFT). The alpha band was defined from 8 to 13 Hz, the absolute alpha power was defined as the area under the PSD curve. The alpha blocking effect was defined

as the differences between eyes-closed and eyes-open absolute alpha power. Spearman's correlations between LLE and alpha power were calculated in both eyes conditions. Also, a mixed effect model with the alpha power as a covariate was fitted. Likelihood ratio test was performed to compared the new model against the original model. Lastly, correlation between eyes condition differences in LLE and alpha blocking was assessed.

2.5. Additional source-space analysis

The major statistical analyses described in section 2.4 were based on the complexity measures calculated from the sensor-space EEG signals. Any site effects revealed could only be interpreted as potential differences in the underlying sources. To gather more evidence, source localization of the EEG signals was performed using the exact low-resolution brain electromagnetic tomography (eLORETA; Pascual-Marqui, 2007). It provides unbiased source estimation in the presence of structured noise and allows the localizations of deep structures such as the cingulate cortex. As we did not have the individual T1 MRI scan from the participants, the forward operator was calculated using template MRI head model *fsaverage* available from the MNE-Python package (Gramfort et al., 2013). The reconstructed sources were parcellated according to the Desikan-Killany atlas and the parcels were grouped into 6 different ROIs, including frontal, parietal, temporal, occipital, anterior and posterior cingulate (Desikan et al., 2006; Klein and Tourville, 2012, see Supplementary Table S10). The source time series were then averaged across all voxels in an ROI, LLEs were computed from averaged time series. Similarly, a 3-way $3 \times 6 \times 2$ mixed ANOVA (age group; ROI; eyes condition) was fitted with gender (female or male) as a covariate.

3. Results

3.1. Averaged effects of age group, site and eyes condition

The type III ANOVA results (Supplementary Table S1) shows that the 3 main effects of age group ($F(2, 138) = 6.865, p < .001$), site ($F(3.67, 507.15) = 121.736, p < .001$) and eyes condition ($F(1, 138) = 198.726, p < .001$) were all significant. Post-hoc comparisons were conducted to examine the main effects and guide further analyses on higher order interactions. The pairwise comparisons between age group (Supplementary Table S2) showed that the averaged LLE of young ($t(138) = 3.703, p < .001$) and young-old ($t(138) = 2.598, p = .021$) group were significantly higher than that of old-old group. Notably, the averaged LLE was not significantly different between the young and young-old group ($t(138) = 1.398, p = .164$). Pairwise comparisons (Supplementary Table S3) showed that the grand-averaged LLE was significantly lower ($t(138) = -14.097, p < .001$) in eyes-open than eyes-closed condition. The main effect of site was illustrated by the averaged LLE topographies shown in Fig. 2b–c. In brief, the LLEs were similar within two groups of sites: (1) FC, CP and PO; (2) PF, LT and RT, with the LLEs of the latter group being lower than those of the former group. Besides the significant main effects, the highest order significant interactions were two 3-way interactions, with the first between age group, eyes condition, and site, and the second between gender, eyes condition and site. Since gender effect is not the primary interest of the present study, the focus was on the first interaction.

3.2. Interaction between age group, eyes condition and site

The 3-way interaction between age group, eyes condition and site (Supplementary Table S1) was significant ($F(6.07, 418.52) = 3.029, p = .006$). From the interaction plot shown in Fig. 3a–b, obvious age-related reductions were present in both eyes conditions as the three lines were separated by an observable margin. Generally, LLE would decrease as age increased, but the differences depended on the site, which contributed to the interaction effect. For example, in eyes-open condition, only

in LT and RT site were the LLEs of young-old group similar to the young group. Also, as reported above, the averaged LLEs were higher in eyes-closed than eyes-open condition.

To address our major question on how LLE is modulated by ageing, we followed up by a 2-way ANOVA in each eyes condition (Supplementary Table S4). Significant age group by site interaction was found in both eyes-open ($F(6.48, 456.89) = 4.596, p = .001$) and eyes-closed conditions ($F(7.49, 528.19) = 2.407, p = .017$). Follow-up 1-way ANOVA revealed significant or marginally significant simple main effects of age group (Supplementary Table S5) in most of the ROIs except in the PO site for both eyes-open ($F(2, 141) = 1.141, p = .322$) and eyes-closed conditions ($F(2, 141) = 1.465, p = .235$). The age group main effect was marginally significant only for LT of eyes-open condition ($F(2, 141) = 2.615, p = .077$) and RT of eyes-closed condition ($F(2, 141) = 2.416, p = .093$). Pairwise comparisons on estimated marginal means from the 3-way ANOVA model were conducted.

In eyes-open condition (Fig. 3c, Supplementary Table S6), the young group showed significantly higher LLE than the old-old group in PF ($p < .001$) and FC ($p < .001$), while such differences were only marginally significant in LT ($p = .081$) and RT ($p = .059$). Between young and young-old adults, significantly higher LLE in the young group was again found in PF ($p = .021$) and FC ($p = .014$), but LLEs in both temporal sites did not differ significantly. Among older adults, the young-old group was found to possess significantly higher LLE than old-old group in PF ($p < .001$) and FC ($p = .009$), while such differences were only marginally significant in LT ($p = .084$) and RT ($p = .059$). In eyes-closed condition (Fig. 3d, Supplementary Table S7), the young group showed significantly higher LLE than the old-old group in PF ($p = .003$), FC ($p = .003$), CP ($p = .021$) and LT ($p = .003$), such difference was marginally significant in RT ($p = .075$). Between young and young-old adults, significantly higher LLE in young adults was only found in FC ($p = .049$). Among older adults, the young-old group exhibited significantly higher LLE than the older-old group in PF ($p = .017$), and LT ($p = .006$), such difference was marginally significant in RT ($p = .098$).

The Spearman's rank correlations between alpha power and LLE within different age groups and eyes conditions were shown in Supplementary Fig. S2. Significant correlations were found only in eyes-open condition: in the young group, significant correlation was found in the CP site ($\rho = .450, p = .004$); in the old-old group, significant correlations were found in CP ($\rho = .630, p = .003$) and PO ($\rho = .570, p = .010$) sites. The likelihood ratio test comparing the original and the updated mixed effect model with alpha power as covariate (Supplementary Table S8) showed no significant improvement. Concerning the alpha blocking effect, no significant correlation between eyes condition differences in LLE and alpha blocking effect were found (Supplementary Table S9).

3.3. Additional source-space analysis

The results of the source-space ANOVA were shown in Supplementary Tables S11–13. Corresponding interaction plots and post-hoc pairwise compairsons results were shown in Supplementary Fig. S3. The result was consistent with our sensor-space findings in that the 3-way interaction between age group, ROI and eyes condition was also significant ($F(4.91, 338.56) = 3.829, p = .002$). In eyes-open condition, the old-old group showed significantly lower LLE than both the young ($p = .005$) and young-old groups ($p = .008$) in the frontal ROI, while no significant differences were found between young and young-old group. Significant differences between young group and both young-old (eyes-open: $p = .057$; eyes-closed: $p = .009$) and old-old groups (eyes-open: $p = .027$; eyes-closed: $p = .001$) were found in the posterior cingulate.

3.4. Correlation between age and complexity measures

Correlation analysis between age and complexity measures was conducted to examine the age-related trends of complexity measures as
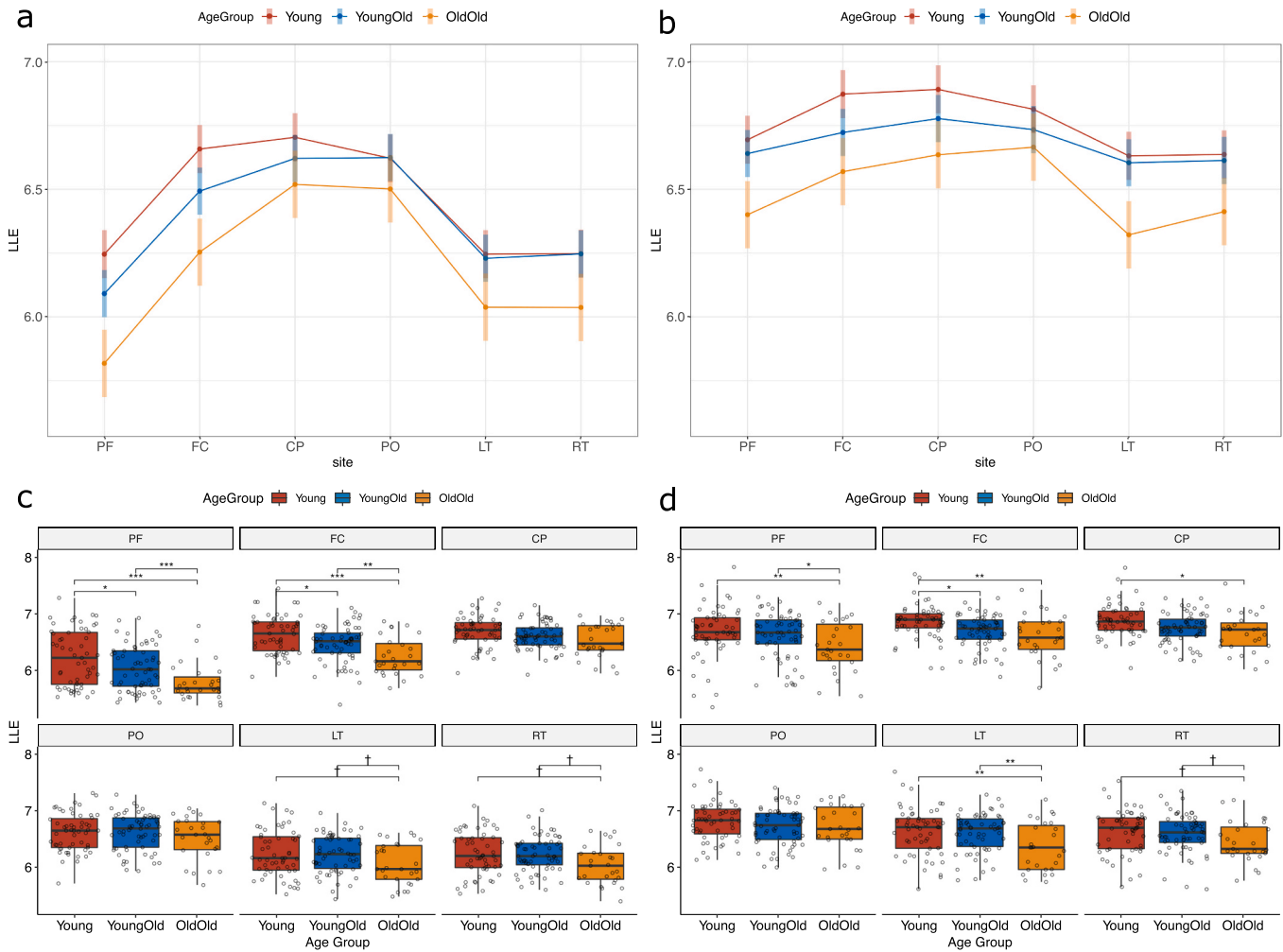
Fig. 3. Interaction plots by eyes condition and post-hoc comparison results. **a,** Interaction plot in eyes-open condition, each point corresponds to the estimated marginal means of each age group in each region, shaded intervals indicate the 95% confidence intervals of each estimate. **b,** Same as **a** but in eyes-closed condition. **c,** Post-hoc comparisons of LLE between age groups in eyes-open condition. Jittering was applied horizontally to improve clarity. **d,** same as **c** but in eyes-closed condition. **c** and **d** were further divided into six subfigures, corresponds to six sites: PF (prefrontal); FC (frontocentral); CP (centroparietal); PO (parieto-occipital); LT (left temporal); RT (right temporal). The significance level is described as: (†: $p < .1$, *: $p < .05$, **: $p < .01$, ***: $p < .001$).

well as their sensitivity towards ageing. While the correlations in both young and older adults were calculated, only the results from older adults are reported here since our focus is on ageing. The numerical correlation results in older adults are summarized in Fig. 4a–b, detailed scatter plots and numerical results can be found in Supplementary Figs. S4–7 and Table S14. Results on the young group are provided in Supplementary Figs. S8–11 and Table S15 for reference. In eyes-open condition, significant negative correlation between LLE and age in PF ($p = .027$), FC ($p = .021$) and RT ($p = .024$) could be observed. All other three measures showed positive effect sizes but only 1/f slope showed significant correlation at PF ($p = .037$). In eyes-closed condition, significant correlations were found only in temporal sites. Significant negative correlation was found between LLE and age in LT ($p = .047$) and RT ($p = .003$) sites. On the other hand, LZC ($p = .027$) and SampEn ($p = .029$) was positively correlated with age in RT site.

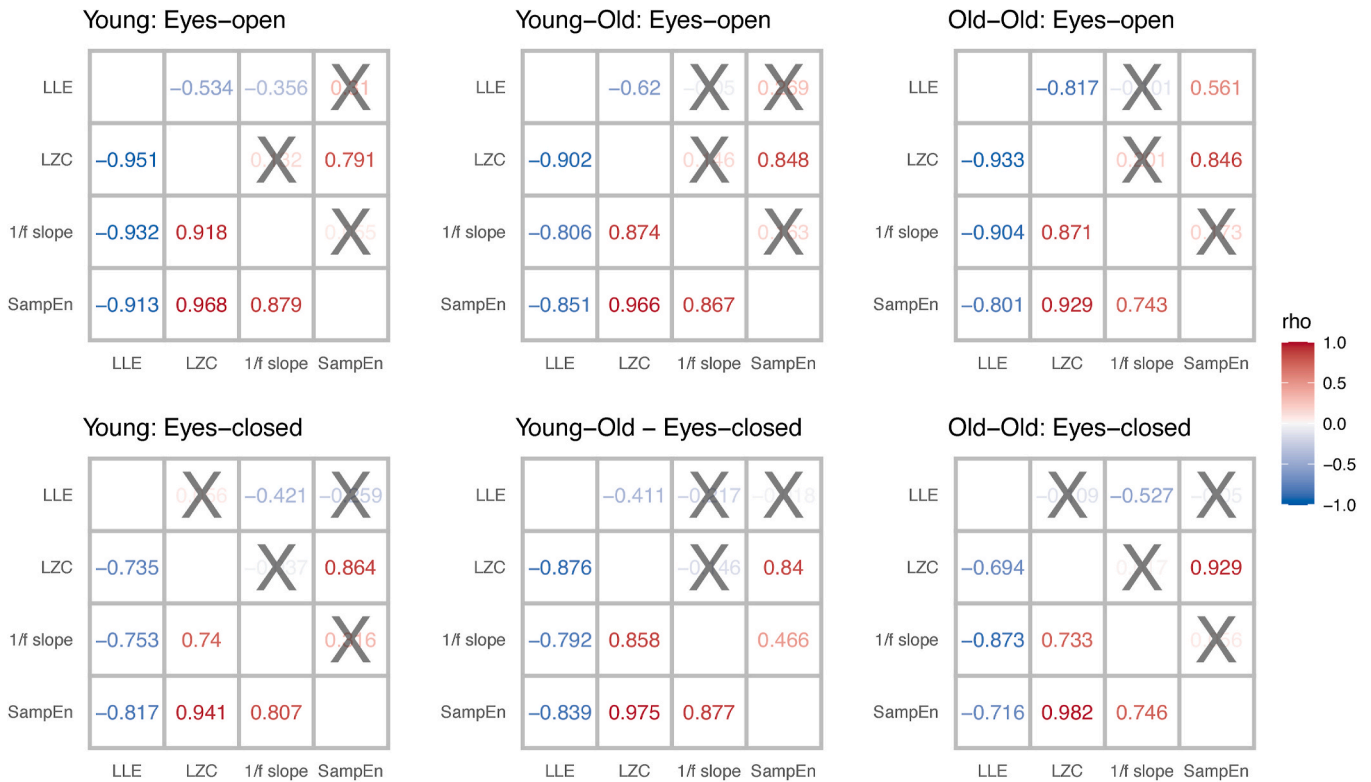### 3.5. Correlation between the complexity measures

Both correlation and partial correlation analyses were conducted to determine the relationship between complexity measures. Fig. 5 showed the correlation matrix between the measures, grouped according to age group and eyes condition, detail numerical results can be found in Supplementary Tables S16–17. The LLE was found to be negatively

correlated ($p < .001$) with all other three complexity measures with high effect sizes (averaged Spearman's ρ across eyes conditions: young: -0.850, young-old: -0.844, old-old: -0.820), while the other three complexity measures were all positively correlated ($p < .001$) with each other (averaged Spearman's ρ across eyes conditions: young: 0.830, young-old: 0.903, old-old: 0.820). The same ANOVA described in section 2.4 was also conducted on LZC as the dependent variable to give a better picture on the opposite patterns between LLE and LZC; the interaction plots and pairwise comparisons results were shown in Supplementary Fig. S12. While the detailed statistics would not be discussed, the patterns of age-related differences were clearly opposite to that of the LLE.

The partial correlation showed different patterns in different populations and eyes conditions. In eyes-open condition, for all three age groups, the negative correlation between LLE and LZC ($p < .001$) and the positive correlation between LZC and SampEn remained significant ($p < .001$) after factoring out other complexity measures. LLE remained negatively correlated with 1/f slope ($p = .03$) only in the young group; SampEn became positively correlated with LLE ($p = .01$) only in the old-old group. In eyes-closed condition, the positive correlation between LZC and SampEn remained significant ($p < .001$) in all three age groups. The correlation pattern of the young group was similar to that of the old-old group. In contrast, the young-old group did not show significant
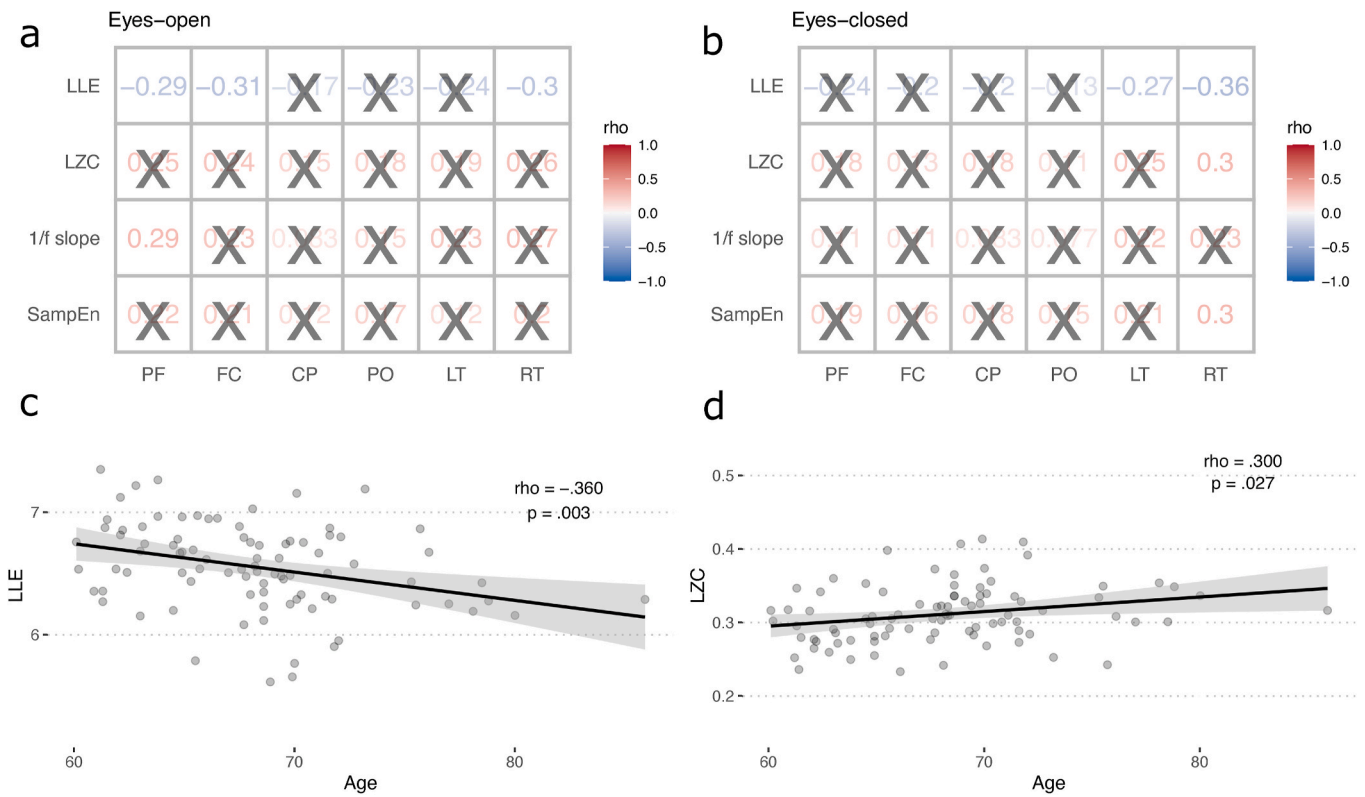
Fig. 4. a, Spearman's rank correlations and significance between age and complexity measures in eyes-open condition, a cross in a cell indicates non-significance ($p > .05$). **b,** same as **a** but in eyes-closed condition. **c,** scatter plot showing the relationship between LLE and age in RT in the eyes-closed condition. The corresponding Spearman's rho and p value is shown on the top right hand corner. **d,** same as **c** but the plot is illustrating the relationship between LZC and age.

Fig. 5. Spearman's rank correlation between complexity measures. Each row corresponds to young, young-old and old-old group from left to right. Each column corresponds to eyes-open and eyes-closed condition from top to bottom. For each correlation matrix, upper triangle: partial correlation; lower triangle: ordinary correlation. A cross in a cell indicates non-significance ($p \leq .05$).

correlation between LLE and 1/f slope as the other two groups. Instead, the negative correlation between LLE and LZC ($p = .004$), and the positive correlation between 1/f slope and SampEn remained significant ($p = .001$), which were not observed in the other two groups.

4. Discussion

4.1. Age-related differences in LLE

Our sensor- and source-space results suggest heterogeneous age-related reduction in LLE across different brain regions. As revealed from the pairwise comparisons results, the degree of reduction could generally be categorized into four different levels. Firstly, the reduction was the most pronounced in prefrontal and frontocentral sites, in the sense that they were more likely to differ between any two of the three age groups. In particular, significant differences among all three groups were found in eyes-open condition. The source-space analysis revealed significant differences in the frontal ROI, suggesting that the sensor-space reduction in frontal sites is originated from the frontal lobe. Secondly, differences were found only between old-old and the other two groups for temporal regions. Specifically, the young-old and old-old group significantly differed in both sensor- and source-space in the eyes-closed condition. No significant differences were observed between young and young-old group regardless of eyes conditions, indicating a relatively less reduction as compared with the frontal lobe. Thirdly, in the parietal and occipital regions, both sensor- and source-space analyses revealed no significant differences between any two of the three age groups, indicating the relatively stable LLEs among age groups. Lastly, the source-space analysis revealed significant differences in LLE between the young and the two old groups, but not between the two older groups in the posterior cingulate. This result suggested a decline in complexity in the deep structure of the brain, and the decline might start from an earlier age before senescence.

For our sensor-space correlation analyses that combined the two older groups, significant negative correlations were found in temporal sites in both eyes conditions (eyes-open: left temporal, eyes-closed: bilateral temporal), while correlations in prefrontal and frontocentral sites were significant only in eyes-open but not eyes-closed condition. Taking together the ANOVAs and the correlation results, the present study suggests that the onset and the degree of decline in prefrontal and frontocentral sites appears to be earlier and more severe than temporal and centroparietal sites. The decline in parieto-occipital site is the slowest in the sense that no significant differences among all three groups can be found regardless of eyes condition. Also, the complexity loss in older adults is more prominently observed in the eyes-open than eyes-closed condition, consistent with a previous study which reported that the functional connectivity was associated with age only in eyes-open but not eyes-closed condition (Agcaoglu et al., 2019). We speculate that it is because the eyes-open condition is a more controlled and demanding condition as compared with eyes-closed condition, which is often related to mind wandering (Mason et al., 2007; Vago and Zeidan, 2016; Diaz et al., 2013).

The most significant complexity loss at prefrontal and frontocentral regions could be related to the structural decline in ageing. In particular, the shrinkage of the frontal lobe was the steepest compared to other lobes (Raz et al., 1997; Dennis and Cabeza, 2008). Our results is consistent with previous structural studies as the most significant reductions were observed in the frontal sites. Integrating with a previous study that revealed the age-related reductions in LLE from infancy to adulthood (Meyer-Lindenberg, 1996), it is possible that the frontal sites show monotonic decline in LLE over the life span without limiting to the age range investigated in the present study. More importantly, the frontal lobe has been extensively studied and regarded as the central hub of executive functions (EF) (Lacreuse et al., 2020). The robust relationship between the prefrontal cortex (PFC) and EF was confirmed by lesion (Alvarez and Emory, 2006) and structural neuroimaging studies

(Yuan and Raz, 2014). The anatomical and functional deterioration of frontal lobe are suggested to be the cause of cognitive deficits in older adults, known as the frontal lobe hypothesis (West, 2000; Cabeza and Dennis, 2013). Also, the source-space analysis revealed significant differences in the posterior cingulate, which is a key region of the default-mode network (DMN). Some previous studies have also reported the relationships between sample entropy and the BOLD activity of posterior cingulate (Yang et al., 2013), as well as the within-network conenctivity of DMN (Mevel et al., 2013). The DMN has been associated with cognitive processes and it is believed to play an important role in suppressing task-unrelated inputs (Grieder et al., 2018). Ageing could reduce the activity in the DMN, its within-network connectivity and in turns affect the cognitive performance of older adults (Mevel et al., 2011, 2013; Hansen et al., 2014). Therefore, we speculate that our results might also reflect the decline in cognitive abilities in older adults. However, further investigation is needed to confirm the connections between LLE and both structural and cognitive factors.

A few previous studies reported relatively stable LLE at the occipital site during development (Meyer-Lindenberg, 1996) and in dementia and AD (Jeong et al, 1998, 2001). In particular, the occipital LLE was not significantly different even between AD patients and normal older adults, while significant decline was observed in other sites. In EEG studies, the occipital alpha is a hallmark of resting-state activities and related to memory, attention and other cognitive abilities (Klimesch, 1999, 2012). It was reported to decline in ageing and cognitive impairment (Babiloni et al., 2015). On the other hand, it has also been connected to visual functions and found to be modulated by sensory input (Webster and Ro, 2020). In fMRI studies, similar activation of visual areas (Aizenstein et al., 2004) and preserved connectivity between left and right visual areas (Andrews-Hanna et al., 2007) between younger and older adults were reported. To investigate if the LLE differences were modulated by the alpha activities, we computed the correlation between alpha power and LLE in each site and eyes conditions. Our results showed significant correlations only in the eyes-open condition, in the CP or PO site of young and old-old groups. Moreover, there were no significant relationship between the alpha blocking and the eyes condition differences in LLE. The above results hence suggested that the age-related differences revealed by LLE were unlikely to be explained by the dominant alpha activities in resting-state. Also, our LLE calculation did not specifically target the alpha band, we suspect that the LLE might reflect the relatively preserved occipital lobe functions of the participants.

4.2. Age-related trend in older adults by different complexity measures

Not all complexity measures revealed significant age-related correlation within older adults. For instance, in the eyes-closed condition, only in temporal sites where LLE, LZC and SampEn were significantly correlated with age. LLE and SampEn showed negative while the LZC showed positive correlations. While inverted U-shaped trajectories of LZC in eyes-closed condition were reported in previous studies (Fernández et al., 2012; Shumbayawonda et al., 2018), the present results suggest a monotonic decrease of LLE from young to old adults. There are two possible reasons that might cause the disagreement. First, the LLE would remain stable or slightly decreasing from young to young-old, and the onset of decline would begin around 60s to 70s. Second, the LLE could exhibit an inverted U-shaped trajectory that peaks before 60s and decreases afterwards, resulting in a similar LLE level of the young and young-old groups. In fact, although the previous study described the age-related trajectory of LZC as an inverted U-shape, the trends in late life most likely remained flat or decreased at a slow rate as the reported peaks were around 60s to 70s of age (Fernández et al., 2012). In particular, they showed that the peak of the trajectory of the right lateral site was at around late 70s, which was the latest among all sites. In the present study, the absence of significant correlation between age and LZC in all sites except RT was therefore not unexpected. In

general, it could be observed that the LLE revealed significant correlations with age in both eyes conditions, while other measures were only sensitive to particular eyes condition. A speculation is that, the LLE was more sensitive than other measures in showing the age-related decline in this age range.

4.3. Interpretation of LLE and relationship between complexity measures

The present study also examined the relationship between common complexity measures. The correlation results showed that the complexity measures were all highly correlated with each other. More precisely, LLE was significantly negatively correlated with other three complexity measures. To our knowledge, there were no similar findings in the literature. The results were highly surprising as these measures were developed from different theoretical backgrounds. The LLE quantifies the rate of divergence of neighboring points in a state space. A lower LLE corresponds to higher predictability of the dynamics, such that one can track the changes of the dynamics for a longer time. In contrast, LZC was developed to quantify randomness (Lempel and Ziv, 1976) and SampEn was usually referred as irregularity (Richman and Moorman, 2000; Jia et al., 2017). The $1/f$ slope of power spectrum is the sign of a critical complex system (He et al., 2010) and was suggested to indicate the signal-to-noise ratio of EEG (Voytek et al., 2015; Faisal et al., 2008). As it is natural to expect coherent relationship between lower predictability and higher irregularity, the significant negative correlation was counter-intuitive as it does not seem possible to become more predictable and more random simultaneously. An explanation can be raised from the fact that LLE is a measure characterizing the dynamics from the reconstructed state space. With the embedding dimension being 20, the LLE was describing the dynamics of 20-dimensional vectors instead of 1-dimensional points. On the other hand, LZC and SampEn were directly calculated from the signal domain, and $1/f$ slope was computed by regression on the power spectrum. As such, the "predictability" quantified by LLE was unlikely to be the same construct as the "irregularity" or "randomness" from other measures qualitatively. Our results indicate that ageing is accompanied by an increase in predictability in the embedded state space and randomness at the signal level. Our results thus support the LOCH by showing that ageing is accompanied by the loss of complexity. More importantly, we showed that the loss of complexity is not only manifested by an one-sided shifting towards regularity or irregularity. Instead, the EEG is more regular as observed in an embedded state space, and meanwhile is more random as observed from the raw signal domain.

Empirically, an important question is whether our highly interrelated correlation results suggest against the recommendation that one should not just rely on a single complexity measure (Goldberger et al., 2002b). We conducted partial correlation analysis to answer the question. The results revealed different correlation patterns in different groups and conditions. For instance, the negative correlation between LLE and SampEn in old-old group in eyes-open condition was flipped to positive after removing the variances from LZC and the $1/f$ slope, while this pattern was not observed in young or young-old group. The implication is that there exists variances that are unique to certain pairs of measures, although they were all highly correlated with each other. Also, the relationships between measures appeared to be modulated by different experimental conditions and populations.

4.4. Limitations and future studies

First, our study is limited by its cross-sectional design. The results were limited to the differences between age groups and the trajectory within a restricted age range of older adults. Including middle-aged adults would be crucial in the future to reveal the full picture of LLE trajectories in ageing. Also, participants of this study were not part of the WEIRD population (Henrich et al., 2010). A complexity trajectory over the life span with the present population would allow one to examine if the trajectory could be generalized across populations. Second, the structural and cognitive correlates of LLE should be explored. This would allow comparisons between trajectories of LLE and other brain structures or cognitive functions (Walhovd et al., 2011; Hartshorne and Germine, 2015). Structurally, the decline in grey matter volume of cortical structures might be very different from that of subcortical structures (Walhovd et al., 2011), it is important to identify the structural correspondence of the declining LLE. On the possible cause of decline, volume reduction in the prefrontal cortex during adolescence was suggested to reflect to the removal of excessive neurons and pruning, while such reduction was related to shrinkage and loss of neurons in ageing (Raz et al., 2005). Identifying potential cognitive correlates of LLE could help to clarify the mechanisms behind the decline in brain structures. Moreover, hypotheses besides the frontal lobe hypothesis (West, 2000) such as the HAROLD (Cabeza, 2002) and PASA (Davis et al., 2008) have predicted regional asymmetries in functional activations, with older adults tending to recruit more frontal and right hemispheric resources as the task demand increases. How EEG complexity is modulated by task demand should be examined in future to provide further evidence for these important hypotheses. Although source localization was performed to gather evidence on the regional effects, it should be noted that the source localization was performed on a 32-channel EEG with a template head model while 64 or more channels is usually recommended (Akalin Acar and Makeig, 2013). The template head model also limited the accuracy of the source localization. Utilizing 64-channel EEG or simultaneous EEG-fMRI could greatly enhance the interpretability of the present study and help investigating the structural and cognitive correlates in the future. Third, the true dimension of EEG signals is never known and can only be determined empirically. Besides time-delay embedding, spatial embedding has also been proven useful for analyzing EEG (Lachaux et al., 1997; Pezard et al., 1998, 1999). The impact of embedding dimensions and other embedding techniques should be further investigated. On the other hand, multiscale variants of complexity have been applied and revealed timescale-dependent patterns in ageing (Sleimen-Malkoun et al., 2015; Labate et al., 2013; Ibáñez-Molina et al., 2015). The connections between LLE and timescale-dependent complexity will be interesting to find out.

5. Conclusion

As revealed by both sensor-space and source-space analyses, the largest Lyapunov exponent (LLE) decreases with age. The decline was found earlier and more severe in frontal region and posterior cingulate than in temporal and occipital regions. Compared with other complexity measures, the LLE possesses high sensitivity towards detecting age-related changes. An important observation was the negative correlation between LLE and other measures. This shows that the loss of complexity in ageing is manifested not only by one-sided shifting towards regularity or irregularity. Instead, the brain signals became simultaneously more regular, as viewed from the perspective of dynamical systems perspective, and more random at raw signal level.

Author contributions

Matthew King-Hang Ma: Conceptualization, Methodology, Formal analysis, Validation, Investigation, Writing - Original Draft, Writing - Review and Editing, Visualization. **Manson Cheuk-Man Fong**: Conceptualization, Formal analysis, Validation, Writing - Review and Editing. **Chenwei Xie**: Conceptualization, Writing - Review and Editing. **Tan Lee**: Conceptualization, Supervision, Writing - Review and Editing. **Guanrong Chen**: Supervision, Writing - Review and Editing. **William Shiyuan Wang**: Supervision, Writing - Review and Editing.

Declaration of competing interest

The authors declare that they have no known competing financial

interests or personal relationships that could have appeared to influence the work reported in this paper.

Acknowledgments

Appendix A. Supplementary data

Supplementary data to this article can be found online at https://doi.org/10.1016/j.ynirp.2021.100054.

References

Abásolo, D., Hornero, R., Espino, P., Alvarez, D., Poza, J., 2006. Entropy analysis of the EEG background activity in Alzheimer's disease patients. Physiol. Meas. 27, 241–253. https://doi.org/10.1088/0967-3334/27/3/003.

Abásolo, D., Hornero, R., Espino, P., Poza, J., Sánchez, C.I., de la Rosa, R., 2005. Analysis of regularity in the EEG background activity of Alzheimer's disease patients with approximate entropy. Clin. Neurophysiol. 116, 1826–1834. https://doi.org/10.1016/j.clinph.2005.04.001.

Aboy, M., Hornero, R., Abásolo, D., Alvarez, D., 2006. Interpretation of the Lempel-Ziv complexity measure in the context of biomedical signal analysis. IEEE (Inst. Electr. Electron. Eng.) Trans. Biomed. Eng. 53, 2282–2288. https://doi.org/10.1109/TBME.2006.883696.

Adeli, H., Ghosh-Dastidar, S., Dadmehr, N., 2007. A wavelet-chaos methodology for analysis of EEGs and EEG subbands to detect seizure and epilepsy. IEEE (Inst. Electr. Electron. Eng.) Trans. Biomed. Eng. 54, 205–211. https://doi.org/10.1109/TBME.2006.886855.

Agcaoglu, O., Wilson, T.W., Wang, Y.P., Stephen, J., Calhoun, V.D., 2019. Resting state connectivity differences in eyes open versus eyes closed conditions. Hum. Brain Mapp. 40, 2488–2498. https://doi.org/10.1002/hbm.24539.

Aizenstein, H.J., Clark, K.A., Butters, M.A., Cochran, J., Stenger, V.A., Meltzer, C.C., Reynolds, C.F., Carter, C.S., 2004. The BOLD hemodynamic response in healthy aging. J. Cognit. Neurosci. 16, 786–793. https://doi.org/10.1162/089892904970681.

Akalin Acar, Z., Makeig, S., 2013. Effects of forward model errors on EEG source localization. Brain Topogr. 26, 378–396. https://doi.org/10.1007/s10548-012-0274-6.

Alvarez, J.A., Emory, E., 2006. Executive function and the frontal lobes: a meta-analytic review. Neuropsychol. Rev. 16, 17–42. https://doi.org/10.1007/s11065-006-9002-x.

Andrews-Hanna, J.R., Snyder, A.Z., Vincent, J.L., Lustig, C., Head, D., Raichle, M.E., Buckner, R.L., 2007. Disruption of large-scale brain systems in advanced aging. Neuron 56, 924–935. https://doi.org/10.1016/j.neuron.2007.10.038.

Anokhin, A.P., Birbaumer, N., Lutzenberger, W., Nikolaev, A., Vogel, F., 1996. Age increases brain complexity. Electroencephalogr. Clin. Neurophysiol. 99, 63–68. https://doi.org/10.1016/0921-884X(96)95573-3.

Babiloni, C., Del Percio, C., Boccardi, M., Lizio, R., Lopez, S., Carducci, F., Marzano, N., Soricelli, A., Ferri, R., Triggiani, A.I., Prestia, A., Salinari, S., Rasser, P.E., Basar, E., Famà, F., Nobili, F., Yener, G., Emek-Savaş, D.D., Gesualdo, L., Mundi, C., Thompson, P.M., Rossini, P.M., Frisoni, G.B., 2015. Occipital sources of resting-state alpha rhythms are related to local gray matter density in subjects with amnesic mild cognitive impairment and Alzheimer's disease. Neurobiol. Aging 36, 556–570. https://doi.org/10.1016/j.neurobiolaging.2014.09.011.

Bates, D., Mächler, M., Bolker, B., Walker, S., 2015. Fitting linear mixed-effects models using lme4. J. Stat. Software 67, 1–48. https://doi.org/10.18637/jss.v067.i01.

Bruce, E.N., Bruce, M.C., Vennelaganti, S., 2009. Sample entropy tracks changes in electroencephalogram power spectrum with sleep state and aging. J. Clin. Neurophysiol. 26, 257–266. https://doi.org/10.1097/WNP.0b013e3181b2f1e3.

Cabeza, R., 2002. Hemispheric asymmetry reduction in older adults: the HAROLD model. Psychol. Aging 17, 85–100. https://doi.org/10.1037/0882-7974.17.1.85.

Cabeza, R., Dennis, N.A., 2013. Frontal lobes and aging. In: Principles of Frontal Lobe Function. Oxford University Press, pp. 628–652. https://doi.org/10.1093/med/9780199837755.003.0044.

Cao, L., 1997. Practical method for determining the minimum embedding dimension of a scalar time series. Phys. Nonlinear Phenom. 110, 43–50. https://doi.org/10.1016/S0167-2789(97)00118-8.

Chialvo, D., 2018. Life at the edge: complexity and criticality in biological function. Acta Phys. Pol. B 49, 1955. https://doi.org/10.5506/APhysPolB.49.1955.

Coffey, D.S., 1998. Self-organization, complexity and chaos: the new biology for medicine. Nat. Med. 4, 882–885. https://doi.org/10.1038/nm0898-882.

Cremer, R., Zeef, E.J., 1987. What kind of noise increases with age? J. Gerontol. 42, 515–518. https://doi.org/10.1523/JNEUROSCI.2332-14.2015.

Dauwels, J., Srinivasan, K., Ramasubba Reddy, M., Musha, T., Vialatte, F.B., Latchoumane, C., Jeong, J., Cichocki, A., 2011. Slowing and loss of complexity in Alzheimer's EEG: two sides of the same coin? Int. J. Alzheimer's Dis. 2011 539621. https://doi.org/10.4061/2011/539621.

Davis, S.W., Dennis, N.A., Daselaar, S.M., Fleck, M.S., Cabeza, R., 2008. Que PASA? the posterior-anterior shift in aging. Cerebr. Cortex 18, 1201–1209. https://doi.org/10.1093/cercor/bhm155.

Dennis, N.A., Cabeza, R., 2008. Neuroimaging of healthy cognitive aging. In: Craik, F.I.M., Salthous, T.A. (Eds.), The Handbook of Aging and Cognition. Psychology Press, pp. 1–54.

Desikan, R.S., Ségonne, F., Fischl, B., Quinn, B.T., Dickerson, B.C., Blacker, D., Buckner, R.L., Dale, A.M., Maguire, R.P., Hyman, B.T., Albert, M.S., Killiany, R.J., 2006. An automated labeling system for subdividing the human cerebral cortex on MRI scans into gyral based regions of interest. Neuroimage 31, 968–980. https://doi.org/10.1016/j.neuroimage.2006.01.021.

Diaz, B.A., Van Der Sluis, S., Moens, S., Benjamins, J.S., Migliorati, F., Stoffers, D., Den Braber, A., Poil, S.S., Hardstone, R., Van't Ent, D., Boomsma, D.I., De Geus, E., Mansvelder, H.D., Van Someren, E.J.W., Linkenkaer-Hansen, K., 2013. The amsterdam Resting-State questionnaire reveals multiple phenotypes of resting-state cognition. Front. Hum. Neurosci. 7, 446. https://doi.org/10.3389/fnhum.2013.00446.

Faisal, A.A., Selen, L.P.J., Wolpert, D.M., 2008. Noise in the nervous system. Nat. Rev. Neurosci. 9, 292–303. https://doi.org/10.1038/nrn2258.

Fernández, A., Zuluaga, P., Abásolo, D., Gómez, C., Serra, A., Méndez, M.A., Hornero, R., 2012. Brain oscillatory complexity across the life span. Clin. Neurophysiol. 123, 2154–2162. https://doi.org/10.1016/j.clinph.2012.04.025.

Goldberger, A.L., Amaral, L.A.N., Hausdorff, J.M., Ivanov, P.C., Peng, C.K., Stanley, H.E., 2002a. Fractal dynamics in physiology: alterations with disease and aging. Proc. Natl. Acad. Sci. Unit. States Am. 99, 2466–2472. https://doi.org/10.1073/pnas.012579499.

Goldberger, A.L., Peng, C.K., Lipsitz, L.A., 2002b. What is physiologic complexity and how does it change with aging and disease? Neurobiol. Aging 23, 23–26. https://doi.org/10.1016/s0197-4580(01)00266-4.

Gramfort, A., Luessi, M., Larson, E., Engemann, D.A., Strohmeier, D., Brodbeck, C., Goj, R., Jas, M., Brooks, T., Parkkonen, L., Hämäläinen, M., 2013. MEG and EEG data analysis with MNE-Python. Front. Neurosci. 7, 267. https://doi.org/10.3389/fnins.2013.00267.

Grieder, M., Wang, D.J.J., Dierks, T., Wahlund, L.O., Jann, K., 2018. Default mode network complexity and cognitive decline in mild Alzheimer's disease. Front. Neurosci. 12, 770. https://doi.org/10.3389/fnins.2018.00770.

Hansen, N.L., Lauritzen, M., Mortensen, E.L., Osler, M., Avlund, K., Fagerlund, B., Rostrup, E., 2014. Subclinical cognitive decline in middle-age is associated with reduced task-induced deactivation of the brain's default mode network. Hum. Brain Mapp. 35, 4488–4498. https://doi.org/10.1002/hbm.22489.

Hartshorne, J.K., Germine, L.T., 2015. When does cognitive functioning peak? the asynchronous rise and fall of different cognitive abilities across the life span. Psychol. Sci. 26, 433–443. https://doi.org/10.1177/0956797614567339.

He, B.J., Zempel, J.M., Snyder, A.Z., Raichle, M.E., 2010. The temporal structures and functional significance of scale-free brain activity. Neuron 66, 353–369. https://doi.org/10.1016/j.neuron.2010.04.020.

Henrich, J., Heine, S.J., Norenzayan, A., 2010. Most people are not WEIRD. Nature 466, 29. https://doi.org/10.1038/466029a.

Holm, S., 1979. A simple sequentially rejective multiple test procedure. Scandinavian.J. Stat. Theory Appl. 6, 65–70. https://doi.org/10.2307/4615733.

Ibáñez-Molina, A.J., Iglesias-Parro, S., Soriano, M.F., Aznarte, J.I., 2015. Multiscale Lempel-Ziv complexity for EEG measures. Clin. Neurophysiol. 126, 541–548. https://doi.org/10.1016/j.clinph.2014.07.012.

Jeong, J., 2004. EEG dynamics in patients with Alzheimer's disease. Clin. Neurophysiol. 115, 1490–1505. https://doi.org/10.1016/j.clinph.2004.01.001.

Jeong, J., Chae, J.H., Kim, S.Y., Han, S.H., 2001. Nonlinear dynamic analysis of the EEG in patients with Alzheimer's disease and vascular dementia. J. Clin. Neurophysiol. 18, 58–67. https://doi.org/10.1097/00004691-200101000-00010.

Jeong, J., Kim, S.Y., Han, S.H., 1998. Non-linear dynamical analysis of the EEG in Alzheimer's disease with optimal embedding dimension. Electroencephalogr. Clin. Neurophysiol. 106, 220–228. https://doi.org/10.1016/s0013-4694(97)00079-5.

Jia, Y., Gu, H., Luo, Q., 2017. Sample entropy reveals an age-related reduction in the complexity of dynamic brain. Sci. Rep. 7, 7990. https://doi.org/10.1038/s41598-017-08565-y.

Khoa, T.Q.D., Huong, N.T.M., Toi, V.V., 2012. Detecting epileptic seizure from scalp EEG using Lyapunov spectrum. Comput. Math. Methods Med 2012, 847686. https://doi.org/10.1155/2012/847686.

Klein, A., Tourville, J., 2012. 101 labeled brain images and a consistent human cortical labeling protocol. Front. Neurosci. 6, 171. https://doi.org/10.3389/fnins.2012.00171.

Klimesch, W., 1999. EEG alpha and theta oscillations reflect cognitive and memory performance: a review and analysis. Brain Res. Rev. 29, 169–195. https://doi.org/10.1016/S0165-0173(98)00056-3.

Klimesch, W., 2012. α-band oscillations, attention, and controlled access to stored information. Trends Cognit. Sci. 16, 606–617. https://doi.org/10.1016/j.tics.2012.10.007.

Krakovská, A., Mezeiová, K., Budáčová, H., 2015. Use of false nearest neighbours for selecting variables and embedding parameters for state space reconstruction. J. Syst. Sci. Complex.2015. https://doi.org/10.1155/2015/932750.

Kyriazis, M., 2003. Practical applications of chaos theory to the modulation of human ageing: nature prefers chaos to regularity. Biogerontology 4, 75–90. https://doi.org/10.1023/a:1023306419861.

Labate, D., Foresta, F.L., Morabito, G., Palamara, I., Morabito, F.C., 2013. Entropic measures of EEG complexity in Alzheimer's disease through a multivariate multiscale approach. IEEE Sensor. J. 13, 3284–3292. https://doi.org/10.1109/JSEN.2013.2271735.

Lachaux, J.P., Pezard, L., Garnero, L., Pelte, C., Renault, B., Varela, F.J., Martinerie, J., 1997. Spatial extension of brain activity fools the single-channel reconstruction of

EEG dynamics. Hum. Brain Mapp. 5, 26–47. https://doi.org/10.1002/(SICI)1097-0193(1997)5:1<26::AID-HBM4>3.0.CO;2-P.

Lacreuse, A., Raz, N., Schmidtke, D., Hopkins, W.D., Herndon, J.G., 2020. Age-related decline in executive function as a hallmark of cognitive ageing in primates: an overview of cognitive and neurobiological studies. Phil. Trans. Biol. Sci. 375, 20190618. https://doi.org/10.1098/rstb.2019.0618.

Lempel, A., Ziv, J., 1976. On the complexity of finite sequences. IEEE Trans. Inf. Theor. 22, 75–81. https://doi.org/10.1109/TIT.1976.1055501.

Lenth, R., 2020. Emmeans: estimated marginal means, aka least-squares means. URL: https://CRAN.R-project.org/package=emmeans.R_package_version_1.5.2-1.

Lipsitz, L.A., 2004. Physiological complexity, aging, and the path to frailty. Sci. Aging Knowl. Environ. https://doi.org/10.1126/sageke.2004.16.pe16, 2004, pe16–pe16.

Lipsitz, L.A., Goldberger, A.L., 1992. Loss of 'complexity' and aging. potential applications of fractals and chaos theory to senescence. JAMA 267, 1806–1809. https://doi.org/10.1001/jama.1992.03480130122036.

Mason, M.F., Norton, M.I., Van Horn, J.D., Wegner, D.M., Grafton, S.T., Macrae, C.N., 2007. Wandering minds: the default network and stimulus-independent thought. Science 315, 393–395. https://doi.org/10.1126/science.1131295.

McBride, J.C., Zhao, X., Munro, N.B., Smith, C.D., Jicha, G.A., Hively, L., Broster, L.S., Schmitt, F.A., Kryscio, R.J., Jiang, Y., 2014. Spectral and complexity analysis of scalp EEG characteristics for mild cognitive impairment and early Alzheimer's disease. Comput. Methods Progr. Biomed. 114, 153–163. https://doi.org/10.1016/j.cmpb.2014.01.019.

Mevel, K., Chételat, G., Eustache, F., Desgranges, B., 2011. The default mode network in healthy aging and Alzheimer's disease. Int. J.Alzheimer's Dis 2011 535816. https://doi.org/10.4061/2011/535816.

Mevel, K., Landeau, B., Fouquet, M., La Joie, R., Villain, N., Mézenge, F., Perrotin, A., Eustache, F., Desgranges, B., Chételat, G., 2013. Age effect on the default mode network, inner thoughts, and cognitive abilities. Neurobiol. Aging 34, 1292–1301. https://doi.org/10.1016/j.neurobiolaging.2012.08.018.

Meyer-Lindenberg, A., 1996. The evolution of complexity in human brain development: an EEG study. Electroencephalogr. Clin. Neurophysiol. 99, 405–411. https://doi.org/10.1016/s0013-4694(96)95699-0.

Müller, V., Lindenberger, U., 2012. Lifespan differences in nonlinear dynamics during rest and auditory oddball performance. Dev. Sci. 15, 540–556. https://doi.org/10.1111/j.1467-7687.2012.01153.x.

Pascual-Marqui, R.D., 2007. Discrete, 3D Distributed, Linear Imaging Methods of Electric Neuronal Activity. Part 1: Exact, Zero Error Localization arXiv:0710.3341.

Pezard, L., Lachaux, J.P., Thomasson, N., Martinerie, J., 1999. Why bother to spatially embed EEG? comments on pritchard et al. Psychophysiology 33, 362–368. https://doi.org/10.1017/s0048577299971822, 1996. Psychophysiology 36, 527–531.

Pezard, L., Martinerie, J., Varela, F.J., Bouchet, F., Guez, D., Derouesné, C., Renault, B., 1998. Entropy maps characterize drug effects on brain dynamics in Alzheimer's disease. Neurosci. Lett. 253, 5–8. https://doi.org/10.1016/s0304-3940(98)00603-x.

Pierce, T.W., Kelly, S.P., Watson, T.D., Replogle, D., King, J.S., Pribram, K.H., 2000. Age differences in dynamic measures of EEG. Brain Topogr. 13, 127–134. https://doi.org/10.1023/a:1026659102713.

Pierce, T.W., Watson, T.D., King, J.S., Kelly, S.P., Pribram, K.H., 2003. Age differences in factor analysis of EEG. Brain Topogr. 16, 19–27. https://doi.org/10.1023/A:1025654331788.

Pritchard, W.S., Duke, D.W., Coburn, K.L., 1991. Altered EEG dynamical responsivity associated with normal aging and probable Alzheimer's disease. Dement. Geriatr. Cognit. Disord. 2, 102–105. https://doi.org/10.1159/000107183.

R Core Team, 2020. R: A Language and Environment for Statistical Computing. R Foundation for Statistical Computing, Vienna, Austria. URL: https://www.R-project.org/.

Raz, N., Gunning, F.M., Head, D., Dupuis, J.H., McQuain, J., Briggs, S.D., Loken, W.J., Thornton, A.E., Acker, J.D., 1997. Selective aging of the human cerebral cortex observed in vivo: differential vulnerability of the prefrontal gray matter. Cerebr. Cortex 7, 268–282. https://doi.org/10.1093/cercor/7.3.268.

Raz, N., Lindenberger, U., Rodrigue, K.M., Kennedy, K.M., Head, D., Williamson, A., Dahle, C., Gerstorf, D., Acker, J.D., 2005. Regional brain changes in aging healthy adults: general trends, individual differences and modifiers. Cerebr. Cortex 15, 1676–1689. https://doi.org/10.1093/cercor/bhi044.

Richman, J.S., Moorman, J.R., 2000. Physiological time-series analysis using approximate entropy and sample entropy. Am. J. Physiol. Heart Circ. Physiol. 278, H2039–H2049. https://doi.org/10.1152/ajpheart.2000.278.6.H2039.

Rosenstein, M.T., Collins, J.J., De Luca, C.J., 1993. A practical method for calculating largest Lyapunov exponents from small data sets. Phys. Nonlinear Phenom. 65, 117–134. https://doi.org/10.1016/0167-2789(93)90009-.

Sehl, M.E., Yates, F.E., 2001. Kinetics of human aging: I. rates of senescence between ages 30 and 70 years in healthy people. The Journals of Gerontology Series A: Biological Sciences and Medical Sciences 56, B198–B208. https://doi.org/10.1093/gerona/56.5.b198.

Shumbayawonda, E., Tosun, P.D., Fernández, A., Hughes, M.P., Abásolo, D., 2018. Complexity changes in brain activity in healthy ageing: a permutation Lempel-Ziv complexity study of magnetoencephalograms. Entropy 20. https://doi.org/10.3390/e20070506.

Sleimen-Malkoun, R., Perdikis, D., Müller, V., Blanc, J.L., Huys, R., Temprado, J.J., Jirsa, V.K., 2015. Brain dynamics of aging: multiscale variability of EEG signals at rest and during an auditory oddball task. eNeuro 2. https://doi.org/10.1523/ENEURO.0067-14.2015.

Sleimen-Malkoun, R., Temprado, J.J., Hong, S.L., 2014. Aging induced loss of complexity and dedifferentiation: consequences for coordination dynamics within and between brain, muscular and behavioral levels. Front. Aging Neurosci. 6, 140. https://doi.org/10.3389/fnagi.2014.00140.

Stam, C.J., Jelles, B., Achtereekte, H.A., Rombouts, S.A., Slaets, J.P., Keunen, R.W., 1995. Investigation of EEG non-linearity in dementia and Parkinson's disease. Electroencephalogr. Clin. Neurophysiol. 95, 309–317. https://doi.org/10.1016/0013-4694(95)00147-Q.

Stam, K.J., Tavy, D.L., Jelles, B., Achtereekte, H.A., Slaets, J.P., Keunen, R.W., 1994. Non-linear dynamical analysis of multichannel EEG: clinical applications in dementia and Parkinson's disease. Brain Topogr. 7, 141–150. https://doi.org/10.1007/BF01186772.

Takens, F., 1981. Detecting strange attractors in turbulence. In: Lecture Notes in Mathematics. Springer Berlin Heidelberg, pp. 366–381. https://doi.org/10.1007/BFb0091924.

Vago, D.R., Zeidan, F., 2016. The brain on silent: mind wandering, mindful awareness, and states of mental tranquility. Ann. N. Y. Acad. Sci. 1373, 96–113. https://doi.org/10.1111/nyas.13171.

Voytek, B., Kramer, M.A., Case, J., Lepage, K.Q., Tempesta, Z.R., Knight, R.T., Gazzaley, A., 2015. Age-Related changes in 1/f neural electrophysiological noise. J. Neurosci. 35, 13257–13265. https://doi.org/10.1523/JNEUROSCI.2332-14.2015.

Walhovd, K.B., Westlye, L.T., Amlien, I., Espeseth, T., Reinvang, I., Raz, N., Agartz, I., Salat, D.H., Greve, D.N., Fischl, B., Dale, A.M., Fjell, A.M., 2011. Consistent neuroanatomical age-related volume differences across multiple samples. Neurobiol. Aging 32, 916–932. https://doi.org/10.1016/j.neurobiolaging.2009.05.013.

Webster, K., Ro, T., 2020. Visual modulation of resting state α oscillations. eNeuro 7. https://doi.org/10.1523/ENEURO.0268-19.2019.

West, R., 2000. In defense of the frontal lobe hypothesis of cognitive aging. J. Int. Neuropsychol. Soc. 6, 727–729. https://doi.org/10.1017/S1355617700666109.

Wolf, A., Swift, J.B., Swinney, H.L., Vastano, J.A., 1985. Determining Lyapunov exponents from a time series. Phys. Nonlinear Phenom. 16, 285–317. https://doi.org/10.1016/0167-2789(85)90011-9.

Wong, A., Law, L.S.N., Liu, W., Wang, Z., Lo, E.S.K., Lau, A., Wong, L.K.S., Mok, V.C.T., 2015. Montreal cognitive assessment: one cutoff never fits all. Stroke 46, 3547–3550. https://doi.org/10.1161/STROKEAHA.115.011226.

Wong, A., Xiong, Y.Y., Kwan, P.W.L., Chan, A.Y.Y., Lam, W.W.M., Wang, K., Chu, W.C. W., Nyenhuis, D.L., Nasreddine, Z., Wong, L.K.S., Mok, V.C.T., 2009. The validity, reliability and clinical utility of the Hong Kong montreal cognitive assessment (HK-MoCA) in patients with cerebral small vessel disease. Dement. Geriatr. Cognit. Disord. 28, 81–87. https://doi.org/10.1159/000232589.

Yang, A.C., Huang, C.C., Yeh, H.L., Liu, M.E., Hong, C.J., Tu, P.C., Chen, J.F., Huang, N. E., Peng, C.K., Lin, C.P., Tsai, S.J., 2013. Complexity of spontaneous BOLD activity in default mode network is correlated with cognitive function in normal male elderly: a multiscale entropy analysis. Neurobiol. Aging 34, 428–438. https://doi.org/10.1016/j.neurobiolaging.2012.05.004.

Yuan, P., Raz, N., 2014. Prefrontal cortex and executive functions in healthy adults: a meta-analysis of structural neuroimaging studies. Neurosci. Biobehav. Rev. 42, 180–192. https://doi.org/10.1016/j.neubiorev.2014.02.005.

Zappasodi, F., Marzetti, L., Olejarczyk, E., Tecchio, F., Pizzella, V., 2015. Age-related changes in electroencephalographic signal complexity. PloS One 10, e0141995. https://doi.org/10.1023/a:1026659102713.